

# QUANTUM EFFICIENCY IMPROVEMENT OF POLARIZED ELECTRON SOURCE USING STRAIN COMPENSATED SUPER LATTICE PHOTOCATHODE

N. Yamamoto\*, X.G. Jin, M. Yamamoto, KEK, Tsukuba, Japan  
T. Miyauchi, A. Mano, M. Hosaka, Y. Takashima, Nagoya University, Aichi, Japan  
Y. Takeda, Advanced Science and Technology Foundation, Aichi, Japan

## Abstract

In order to improve the quantum efficiency (QE) of the NEA-GaAs based polarized electron source. GaAs/GaAsP strain-compensated superlattice (SL) samples with thickness up to 720 nm were fabricated and an electron spin polarization (ESP) of 92 % and QE of 1.6 % were achieved at the pump laser energy of 1.59 eV for an 196nm-thickness sample. Furthermore, as results of the spin-resolved analyses, a slightly degradation of the crystalline quality for thicker thickness samples were indicated, however the effect for the beam performance was negligible up to the thickness of 720 nm. Then it is confirmed that the ESP is limited by the spin relaxation effect during electron transport in the semiconductor for the thicker thickness strain-compensated SLs.

## INTRODUCTION

The GaAs-type semiconductor photocathode (PC) with a negative electron affinity (NEA) surface is used as a conventionally polarized electron source (PES). Recently, highly polarized electron beams produced by the NEA-GaAs PCs have been widely applied as a source for electron microscopes, such as a low energy electron microscopy (SPLEEM) [1] and a transmission electron microscopy (Spin-TEM) [2]. For applications in future high energy accelerators, generation of highly polarized and intense electron beam is an important technology. The International Linear Collider (ILC) requires an electron beam with > 80% electron spin polarization (ESP) and a bunch charge of 4.8 nC at the exit of the gun [3]. For the electron-ion collider at BNL, same polarization and an average current of 50 mA are required [4].

To answer these needs of future high energy accelerators, we have developed the polarized electron source for more than twenty years, and the GaAs/GaAsP strained superlattice (SL) PC was developed and demonstrated the ESP of around 90% and the quantum efficiency (QE) of 0.5% by using reflected type [5] and transmission type [6] PCs. As the NEA-type PCs have an intrinsic advantage for the beam emittance [7], high brightness beam with high ESP could be obtained [8]. However, the beam brightness is limited practically by the lack of QE value. Furthermore, to realize high intense beam required by future high energy accelerators, the QE improvement becomes important.

Recently, we have developed the strain-compensated SL PCs [9]. In the strained SL structure of conventional strained

Table 1: Design Parameters of PC samples

Parameter	value
Band gap energy	1.54 eV
Cond. band Minimum width	29 meV
Heavy hole (HH) band Width	< 1 meV
Light hole (LH) band Width	29 meV
Band Split between HH and LH	75 meV

SL PCs, increasing SL layer thickness causes strain accumulation, resulting in the introduction of defects. Then the crystalline quality becomes worse and the SL thickness is limited. To overcome this problem, the use of a strain-compensated SL has been proposed. In such a structure, an opposing strain is introduced in the barrier layers to offset the strain in the quantum well layers so that no critical thickness limitation exists on the overall thickness of the SL structure and high crystalline quality is expected.

To demonstrate this effect of the strain-compensated SL PC, GaAs/GaAsP strain-compensated SL PCs have been developed and PC samples with the SL thickness from 96 to 720 nm were fabricated on the AlGaAsP buffer layer. Furthermore, in the measurements, the ESP of 92 % and the QE of 1.6 % were achieved by using the 192 nm sample [10].

In this paper, we reported the details of the GaAs/GaAsP strain-compensated SL PCs and discussed the thickness dependence of the crystalline parameter, such as an energy gap, a band width and a band split value between heavy hole and light hole bands at the valence-band maximum.

## DESIGN OF STRAIN-COMPENSATED SL

GaAs/GaAsP strain-compensated SL samples were fabricated using a low-pressure metal organic vapor phase epitaxy (MOVPE) system with a vertical cold-wall quartz reactor. The 12-, 24-, 36-, 60- and 90-pair GaAs/GaAs<sub>0.62</sub>P<sub>0.38</sub> strain-compensated SL layers were grown with a 500-nm thick Al<sub>0.1</sub>Ga<sub>0.9</sub>As<sub>0.81</sub>P<sub>0.19</sub> buffer layer and GaP substrate. The thickness of the each SL layer was 4 nm.

In the above configuration, the designed SL parameters could be calculated and shown in Table 1. The band gap energy is set to be 1.54 eV and lower than that of the buffer and substrate materials. Then the pump laser could be also irradiated the SL layers from the substrate side (transmission PC). The band width of heavy hole (HH) and Light hole (LH) minibands at the valence-band maximum are less than 1 meV and are 29 meV, respectively. The band split value between

\* naoto.yamamoto@kek.jp

Content from this work may be used under the terms of the CC BY 3.0 licence (© 2015). Any distribution of this work must maintain attribution to the author(s), title of the work, publisher, and DOI.

HH and LH minibands is important to obtain high ESPs and is calculated to be 75 meV. In our previous study [11], [12], this band split value is sufficient for high ESPs.

## EXPERIMENTAL RESULTS

The ESPs and QEs were measured with the energy range between 1.47 and 1.78 eV. For the measurement of the ESPs, the 100keV-mott polarimeter [13] and transmission-type electron gun [8] were employed at Nagoya University. Then all ESP values shown in this paper were measured with the back-side laser irradiation (transmission mode). The CW Ti:sapphire laser was used as a pump laser and the bandwidth was smaller than 1 nm. Before the NEA process, the samples were processed by the heating cleaning (HC), and some samples were also processed with the atomic hydrogen [14]. Before and After the atomic hydrogen cleaning (AHC) process, the behaviors of QE spectra were not changed and showed two distinct steps near 1.64 and 1.74 eV. The lower step corresponds to the threshold of the energy gap between LH band and the conduction band minimum (CBM) and the higher one to the gap between HH and CBM. The clear step QE spectra are important proof that the GaAs/GaAsP strain-compensated SLs are high crystalline quality. In addition, we considered that the SL layers of the samples were not damaged by the AHC process.

The measured ESPs and QEs with different SL thickness are shown in Fig. 1. In Fig. 1, the open circles represent the maximum ESP in the measurement energy range. For the QEs, there are two series of the data with (closed squares) or without (open triangles) the AHC process in Fig. 1.

In Fig. 1, the maximum ESPs around 90 % were obtained until the thickness of 288 nm (36-pair), and thicker than the thickness of 288 nm the ESP values started to decrease slightly. Focusing on the series of QE data with only HC process in Fig. 1, it is found that the QEs is proportion to the SL thickness. It means that the life time of the excited electrons is much longer than the transport time, and the emitted electrons in thicker sample should transport longer distance. Furthermore, we employed the AHC process for the 12- and 24-pair SL samples and the drastically improvement of QEs was observed. Especially for the 24-pair SL sample, an ESP of 92 % and QE of 1.6 % were obtained at the pump laser energy of 1.59 eV. In precise, although the different electron gun systems were used for the ESP and QE measurements, we considered that both performances could be simultaneously achieved because there are no technical difference for each electron gun system.

## DISCUSSION

For detailed analyses, spin-resolved QE spectra were derived [8]. The spectra were reduced using the following definition formula:  $Q_L = QE(1 + ESP)/2$  and  $Q_R = QE(1 - ESP)/2$ , where subscripts L and R mean left-handed and right-handed electrons. These  $Q_L$  and  $Q_R$  are proportional to the photoabsorption coefficients between the CBM and the HH and LH minibands at the valence-band maxi-

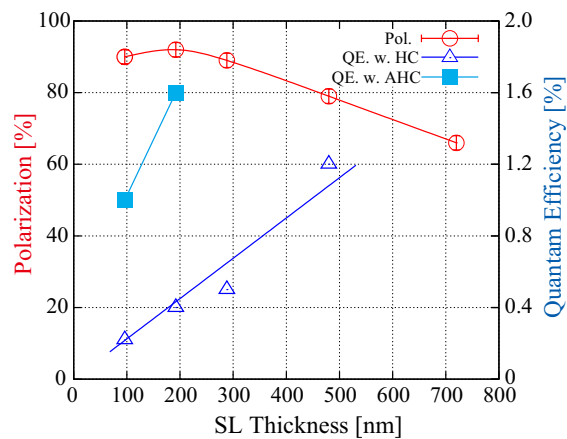


Figure 1: Thickness dependences of the polarization and the QE. The open circles represent the spin ESP. The squares and triangles represent the QE with and without atomic heat cleaning treatment, respectively.

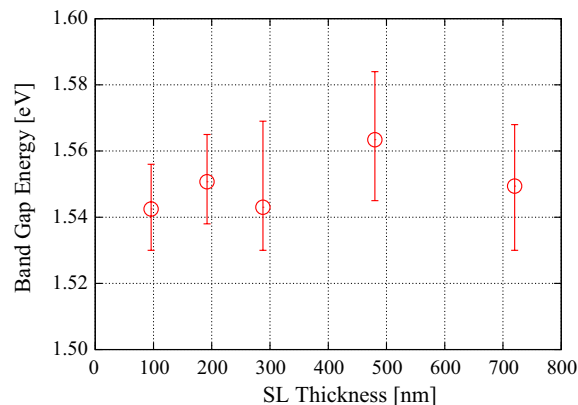


Figure 2: Band gap energy as a function of the SL thickness.

mum. Furthermore, from the obtained  $Q_L$  ( $Q_R$ ) spectra, the band gap energy, band width of each miniband and band split between HH and LH minibands could be derived. The derived values are plotted as functions of the SL thickness in Figs. 2–4. It is noticed that the band width for each miniband are convolved with the CBM band width.

The band gap energies as a function of the SL thickness were shown in Fig. 2. The values exhibits no SL thickness dependence within the analysis accuracy and are consistent with the design value.

The band widths of each miniband as a function of the SL thickness were shown in Fig. 3. The design value of HH miniband width is so small compared with the analysis resolution that the dependence can not be observed. Then increases of the LH miniband width was only observed. The band width for the sample with the 96 thickness agrees with the design value. It is considered that the crystalline quality becomes slightly worse for thicker thickness samples and it causes the band structure to blur.

The band split values as a function of the SL thickness were shown in Fig. 4. The band split values decrease down to 40 meV with SL thickness as a result of the increase of the

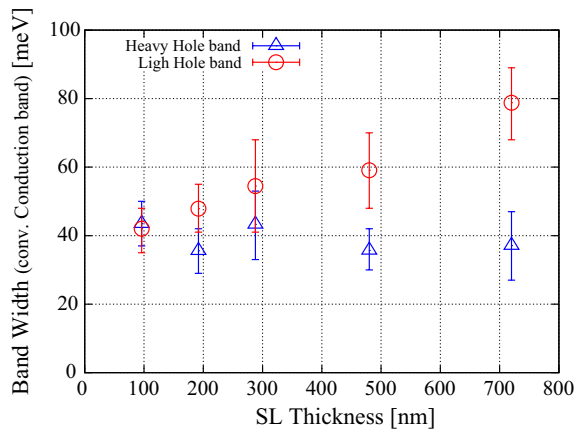


Figure 3: Band widths as a function of the SL thickness. Open circles and triangles indicate the width of LH and HH minibands at the valence-band maximum, respectively.

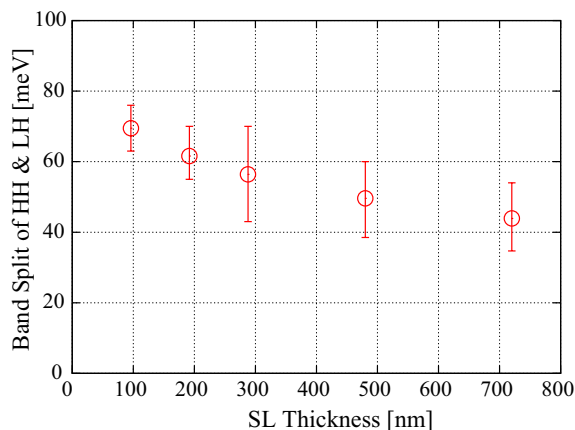


Figure 4: Band split values as a function of the SL thickness.

LH band width. The band split of 40 meV is small compared with the design value, however, it is considered that the effect for the beam performances can be negligible in our measurement condition because the pump laser bandwidth is sufficient small compared with the derived band split. In addition, taking into account the spin relaxation effect during the transport process in the CBM, where the spin relaxation time is estimated to be 140 ps [9], the behavior of ESP degradation shown in Fig. 1 could be reproduced. Then the ESP degradation can be understood as the result of spin relaxation during electron transport.

## CONCLUSION

In order to improve QE performance of PES, we have proposed and developed the strain-compensated SL PCs. In the study, the GaAs/GaAsP strain-compensated samples with the SL thickness from 96 to 720 nm were fabricated and it was confirmed that the QEs increased proportion to the SL thickness. Up to now, the best performance of 92% ESP and 1.6% QE was achieved by the 192nm-thickness SL photocathode.

Furthermore, for the thicker thickness samples, the ESP values started to decrease slightly. The ESP decreases could be understood by considering the spin relaxation during the transport in the semiconductor with the spin relaxation time of 140 ps.

Applying spin-resolved QE analysis for ESP and QE data of various SL thickness samples, a blurring of LH miniband and narrowing of the band split value between HH and LH are speculated. However the band split value even for the 720 nm thickness sample is adequate large compared with the pump laser bandwidth and the effect on the beam performances is considered to be negligible. Then it is concluded that the spin relaxation is dominant effect to limit the ESP values for thicker strain-compensated SL samples.

## ACKNOWLEDGMENT

This work was also supported by the Grants-in-Aid for Scientific Research (A) (23246003) and Grants-in-Aid for Scientific Research (C) (25390066) from the Japan Society for the Promotion of Science (JSPS).

## REFERENCES

- [1] M. Suzuki, M. Hashimoto, T. Yasue, T. Koshikawa, Y. Nakagawa, et al., Appl. Phys. Express 3 (2010) 026601.
- [2] M. Kuwahara, S. Kusunoki, X. G. Jin, T. Nakanishi, Y. Takeda, et al., Appl. Phys. Lett. 101 (3) (2012) 033102.
- [3] ILC technical design report, <https://www.linearcollider.org/ilc/publications/technical-design-report>
- [4] BNL press release on EIC collaboration, <http://www.bnl.gov/rhic/news2/news.asp?a=2870&t=today>
- [5] T. Nishitani, T. Nakanishi, M. Yamamoto, S. Okumi, F. Furuta, et al., J. Appl. Phys. 97 (9) (2005) 94907–94907.
- [6] X. Jin, F. Ichihashi, A. Mano, N. Yamamoto, Y. Takeda, Jpn. J. Appl. Phys. 51 (2012) 108004.
- [7] N. Yamamoto, M. Yamamoto, M. Kuwahara, R. Sakai, T. Morino, et al., J. Appl. Phys. 102 (2) (2007) 024904.
- [8] N. Yamamoto, T. Nakanishi, A. Mano, Y. Nakagawa, S. Okumi, et al., J. Appl. Phys. 103 (6) (2008) 064905.
- [9] X. Jin, A. Mano, F. Ichihashi, N. Yamamoto, Y. Takeda, Appl. Phys. Express 6 (1) (2013) 015801.
- [10] X. Jin, B. Ozdol, M. Yamamoto, A. Mano, N. Yamamoto, et al., Appl. Phys. Lett. 105 (20) (2014) 203509.
- [11] X. Jin, N. Yamamoto, Y. Nakagawa, A. Mano, T. Kato, et al., Appl. Phys. Express 1 (2008) 045002.
- [12] X. Jin, Y. Maeda, T. Saka, M. Tanioku, S. Fuchi, et al., Journal of Crystal Growth 310 (23) (2008) 5039 – 5043.
- [13] T. Nakanishi, K. Dohmae, S. Fukui, Y. Hayashi, I. Hirose, et al., Jpn. J. Appl. Phys. 25 (1986) 766–767.
- [14] M. Yamamoto, K. Wada, T. Nakanishi, S. Okumi, K. Togawa, et al., AIP Conf. Proc. 570 (1) (2001) 1018–1020.